Eur. J. Mineral.
2019, **31**, 1025–1032
Published online 18 September 2019

Elasmochloite, $Na_3Cu_6BiO_4(SO_4)_5$, a new fumarolic mineral from the Tolbachik volcano, Kamchatka, Russia

Igor V. PEKOV[1,*], Sergey N. BRITVIN[2,3], Atali A. AGAKHANOV[4], Marina F. VIGASINA[1] and Evgeny G. SIDOROV[5]

[1]Faculty of Geology, Moscow State University, Vorobievy Gory, 119991 Moscow, Russia
*Corresponding author, e-mail: igorpekov@mail.ru
[2]Department of Crystallography, St. Petersburg State University, University Embankment 7/9, 199034 St. Petersburg, Russia
[3]Kola Science Center of Russian Academy of Sciences, Fersman Str. 14, 184200 Apatity, Russia
[4]Fersman Mineralogical Museum of Russian Academy of Sciences, Leninsky Prospekt 18-2, 119071 Moscow, Russia
[5]Institute of Volcanology and Seismology, Far Eastern Branch of Russian Academy of Sciences, Piip Boulevard 9, 683006 Petropavlovsk-Kamchatsky, Russia

Abstract: The new mineral elasmochloite, $Na_3Cu_6BiO_4(SO_4)_5$, was found in the Arsenatnaya fumarole at the Second scoria cone of the Northern Breakthrough of the Great Tolbachik Fissure Eruption, Tolbachik volcano, Kamchatka, Russia. It is associated with tenorite, hematite, langbeinite, aphthitalite, krasheninnikovite and johillerite. Elasmochloite occurs as lamellar crystals flattened on {001}, up to 0.005 × 0.07 × 0.1 mm in size, separate or combined into open-work clusters up to 0.3 mm across. It is transparent, green, with vitreous lustre. The calculated density (D_{calc}) is 3.844 g cm^{-3}. Elasmochloite is optically uniaxial or pseudo-unixial (−), $\alpha = 1.611(2)$, $\beta = \gamma = 1.698(2)$, $2V \approx 0°$. Pleochroism is strong, $Z \approx Y$ (grass-green) > X (turquoise-blue). The chemical composition obtained by electron-microprobe analysis is (in wt%): Na_2O 6.67, K_2O 0.82, CuO 38.77, ZnO 0.25, PbO 3.17, Bi_2O_3 17.66, SO_3 32.81, total 100.15. The empirical formula based on 24 O atoms per formula unit (*apfu*) is $Na_{2.63}K_{0.21}Cu_{5.96}Zn_{0.04}Pb_{0.17}Bi_{0.93}S_{5.01}O_{24}$. Elasmochloite is monoclinic, $P2_1/n$, *a* 10.1273(9), *b* 10.1193(8), *c* 21.1120(16) Å, β 102.272(8)°, *V* 2114.1(3) Å^3 and *Z* = 4. The strongest reflections of the powder X-ray diffraction (XRD) pattern [*d*, Å(*I*)(*hkl*)] are: 10.33(100)(002), 7.04(18)(110, $\bar{1}$11), 6.33(14)(111, $\bar{1}$12), 3.576(24)($\bar{2}$21), 2.920(14)($\bar{2}$25), 2.529(14)($\bar{4}$02, 040) and 2.460(14)($\bar{2}$27). The crystal-structure model was obtained from single-crystal XRD data, R_1 = 20.6%. It contains two types of alternating polyhedral layers: (1) “copper-bismuth slabs” composed by $[BiO_4O_2]$ polyhedra, $[CuO_5]$ square pyramids and $[CuO_4]$ squares and (2) “sodium slabs” consisting of $[NaO_5]$ and $[NaO_6]$ polyhedra. Corner-sharing $[SO_4]$ tetrahedra integrate cationic polyhedra into the whole structure. In an anion-centred approach, the structure can be expressed as a stacking of perforated layers composed of $[Cu_8BiO_4]$ “half-cube” clusters interleaved with $[SO_4]$ tetrahedra and Na cations. Elasmochloite belongs to a novel structure type but has some common structural features with nabokoite $KCu_7Te^{4+}O_4(SO_4)_5Cl$ and favreauite $PbCu_6BiO_4(Se^{4+}O_3)_4(OH)\cdot H_2O$. The mineral name is based on the Greek words ἔλασμα, lamella, and χλόη, the green shoot, in allusion to the green colour and lamellar crystal habit.

Key-words: elasmochloite; new mineral; sodium copper bismuth sulfate; oxysulfate; crystal structure; fumarole; Tolbachik volcano; Kamchatka.

1. Introduction

In this paper, we describe the 15th representative of a crystal-chemically specific family of minerals, namely hydrogen-free alkali-copper oxysulfates. They contain additional O^{2-} anions non-bound to S^{6+}. This family includes euchlorine $KNaCu_3O(SO_4)_3$ (Scordari & Stasi, 1990), fedotovite $K_2Cu_3O(SO_4)_3$ (Vergasova *et al.*, 1988a; Starova *et al.*, 1991), puninite $Na_2Cu_3O(SO_4)_3$ (Siidra *et al.*, 2017), wulffite $K_3NaCu_4O_2(SO_4)_4$, parawulffite $K_5Na_3Cu_8O_4(SO_4)_8$ (Pekov *et al.*, 2014), kamchatkite $KCu_3O(SO_4)_2Cl$ (Vergasova *et al.*, 1988b; Varaksina *et al.*, 1990; Siidra *et al.*, 2017), piypite, $K_8Cu_9O_4(SO_4)_8Cl_2$ (Effenberger & Zemann, 1984; Vergasova *et al.*, 1984), klyuchevskite $K_3Cu_3Fe^{3+}O_2(SO_4)_4$ (Vergasova *et al.*, 1989; Gorskaya *et al.*, 1992), alumoklyuchevskite $K_3Cu_3AlO_2(SO_4)_4$ (Gorskaya *et al.*, 1995; Krivovichev *et al.*, 2009; Siidra *et al.*, 2017), nabokoite $KCu_7Te^{4+}O_4(SO_4)_5Cl$, atlasovite $KCu_7Fe^{3+}Bi^{3+}O_4(SO_4)_5Cl$ (Popova *et al.*, 1987; Pertlik & Zemann, 1988), eleomelanite $(K_2Pb)Cu_4O_2(SO_4)_4$ (Pekov *et al.*, 2016), cryptochalcite $K_2Cu_5O(SO_4)_5$, cesiodymite $CsKCu_5O(SO_4)_5$ (Pekov *et al.*, 2018b) and the title compound elasmochloite $Na_3Cu_6BiO_4(SO_4)_5$. They are endemics of the oxidizing-type volcanic fumaroles in which

0935-1221/19/0031-2887 $ 3.60
https://doi.org/10.1127/ejm/2019/0031-2887

they deposit directly from hot gas at temperatures not lower than 350–400 °C. All these minerals are known from the Tolbachik volcano, Kamchatka, Russia, which is the type locality for all of them but euchlorine. Data on the crystal chemistry and genetic features of oxysulfates belonging to this family were summarized by Pekov *et al.* (2018c).

The name elasmochloite (Cyrillic: эласмохлоит) is based on the Greek words ἔλασμα, lamella, and χλόη, the green shoot or green grass. In ancient Greek mythology, Chloe ("the green shoot") was one of the titles of Demeter, the goddess of the harvest and agriculture. The mineral is named so in allusion to its green colour and lamellar crystal habit.

Both new mineral and name have been approved by the IMA Commission on New Minerals, Nomenclature and Classification (IMA No. 2018–015). The type specimen is deposited in the systematic collection of the Fersman Mineralogical Museum of the Russian Academy of Sciences, Moscow, with the catalogue number 96203.

2. Occurrence, general appearance and morphology

Elasmochloite was discovered in a single specimen found by us in July 2013 in the Arsenatnaya fumarole located at the summit of the Second scoria cone of the Northern Breakthrough of the Great Tolbachik Fissure Eruption (NB GTFE). This scoria cone, a monogenetic volcano about 300 m high and approximately 0.1 km^3 in volume which formed in 1975 (Fedotov & Markhinin, 1983), is located 18 km SSW of the active volcano Ploskiy Tolbachik in the central part of Kamchatka Peninsula, Far-Eastern Region, Russia. The general description of the Arsenatnaya fumarole has been published by Pekov *et al.* (2018a).

The specimen with the new mineral was collected from the central part of Arsenatnaya at about 1 m depth. The new mineral is associated with tenorite, hematite, langbeinite, aphthitalite, krasheninnikovite and johillerite. The temperature measured in this area during the collecting was 380–400 °C. We believe that elasmochloite was deposited directly from the gas phase as a volcanic sublimate at temperatures not lower than 400 °C.

The new mineral occurs as lamellar crystals, flattened on [001], up to 0.005 × 0.07 × 0.1 mm in size, separate or combined into open-work clusters up to 0.3 mm across, isolated or forming interrupted crusts up to 1 × 1 mm in area overgrowing the surface of basalt scoria altered by fumarolic gas (Figs. 1 and 2). Some crystals are quadratic or rectangular lamellae with cut vertices, *i.e.*, there are octagonal platelets (Fig. 2). This morphological feature probably reflects the pseudo-tetragonal character of the monoclinic crystal structure (see below). The pinacoid {001} is the major crystal form; lateral faces were not indexed.

3. Physical properties and optical data

Elasmochloite is a transparent green mineral. The streak is pale greenish. The lustre is strong vitreous. The mineral is brittle. Cleavage or parting was not observed and the fracture is uneven. The Mohs' hardness and density could not be determined because of the small size of individual crystals and the open-work character of aggregates. The density value calculated from empirical formula is 3.844 g cm^{-3}.

Elasmochloite is optically uniaxial (−), ω = 1.698(2), ε = 1.611(2) (589 nm). Pleochroism is strong, *O* (grass-green) > *E* (turquoise-blue). The mineral is actually monoclinic but possesses pseudo-tetragonal symmetry (see below) which definitely causes its optical properties typical for tetragonal crystals. It could be interpreted alternatively as biaxial, pseudo-uniaxial (−), α = 1.611(2), β = γ = 1.698 (2), 2 *V* ≈ 0°, with the following absorption scheme: *Z* ≈ *Y* (grass-green) > *X* (turquoise-blue).

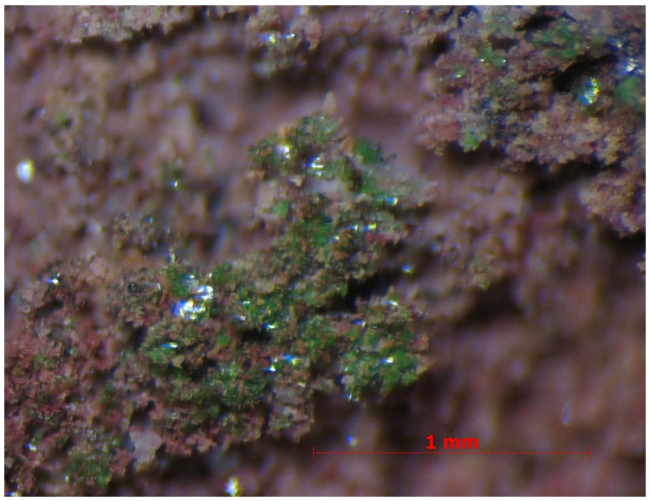

Figure 1. Green crystals of elasmochloite forming clusters and interrupted crusts on the surface of basalt scoria altered by fumarolic gas (the red coloration of some areas of scoria surface is caused by fine-powdery hematite). Field of view: 2.3 mm. Photo: I.V. Pekov & A.V. Kasatkin.

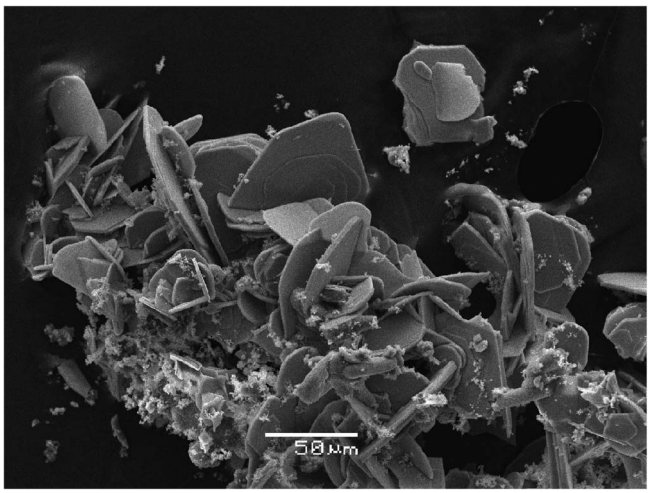

Figure 2. Cluster of lamellar crystals of elasmochloite. Scanning electron microscope image (secondary electrons).

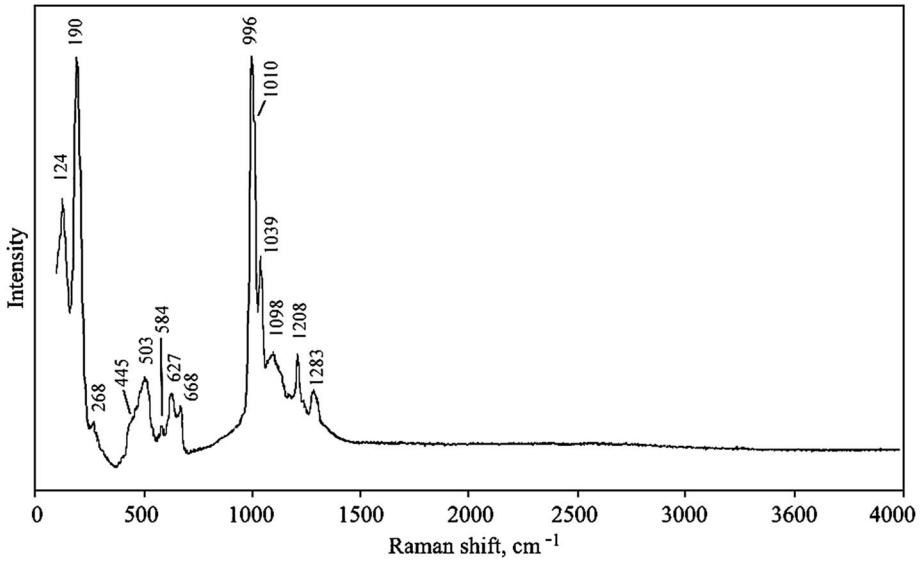

Figure 3. The Raman spectrum of elasmochloite.

4. Raman spectroscopy

The Raman spectrum of elasmochloite (Fig. 3) was obtained using an EnSpectr R532 spectrophotometer with a green laser (532 nm) at room temperature. The output power of the laser beam was about 9 mW. The spectrum was processed using the EnSpectr expert mode program in the range 100–4000 cm^{-1} with the use of a holographic diffraction grating with 1800 mm^{-1} and a resolution equal to 6 cm^{-1}. The diameter of the focal spot on the sample was about 10 μm. The spectrum was obtained for a randomly oriented crystal.

Bands in the Raman spectrum of elasmochloite and their assignments, according to Nakamoto (1986), are (cm^{-1}, s – strong band): 1283 s, 1208, 1098 [$F_2(\nu_3)$-type stretching vibrations of SO_4^{2-}], 1039, 1010s, 996s [$A_1(\nu_1)$ symmetric stretching vibrations of SO_4^{2-}], 668, 627, 584 [$F_2(\nu_4)$ bending vibrations of SO_4^{2-}], 503, 445 [$E(\nu_2)$ bending vibrations of SO_4^{2-}], 268, 190s and 124 (lattice modes). The region between 550 and 250 cm^{-1} can also contain bands corresponding to Bi^{3+}–O and Cu^{2+}–O stretching vibrations.

The absence of bands with frequencies higher than 1300 cm^{-1} indicates the absence of groups with O–H, C–H, C–O, N–H and N–O bonds in elasmochloite.

5. Chemical data

Chemical analyses for elasmochloite were obtained using a Jeol 733 electron microprobe instrument operated in wavelength-dispersive mode with an accelerating voltage of 20 kV, a beam current of 20 nA, and a beam diameter of 3 μm. The chemical composition (average of seven point analyses) is given in Table 1. Contents of other elements with atomic numbers higher than carbon are below detection limits.

The empirical formula calculated (taking into account the crystal-structure data) on the basis of 24 O *apfu* is $Na_{2.63}K_{0.21}Cu_{5.96}Zn_{0.04}Pb_{0.17}Bi_{0.93}S_{5.01}O_{24}$. The simplified formula is $Na_3Cu_6BiO_4(SO_4)_5$, which requires Na_2O 7.72, CuO 39.66, Bi_2O_3 19.36, SO_3 33.26, total 100.00 wt%.

Table 1. Chemical composition of elasmochloite.

Oxide	Wt%	Range	*SD*	Probe standard
Na_2O	6.67	6.50–6.87	0.15	Albite
K_2O	0.82	0.70–0.90	0.07	Microcline
CuO	38.77	38.37–39.34	0.36	Cu
ZnO	0.25	0.00–1.06	0.25	ZnS
PbO	3.17	2.75–3.64	0.35	$PbTiO_3$
Bi_2O_3	17.66	17.17–18.84	0.56	Bi
SO_3	32.81	32.42–33.04	0.25	ZnS
Total	100.15			

The Gladstone-Dale compatibility index (*cf.* Mandarino, 1981) $1 - (K_p/K_c) = -0.026$, excellent.

6. X-ray crystallography

Powder X-ray diffraction (XRD) data of elasmochloite (Table 2) were collected with a Rigaku R-AXIS Rapid II single-crystal diffractometer equipped with a cylindrical image plate detector (Debye-Scherrer geometry; d = 127.4 mm; Co$K\alpha$ radiation). The monoclinic unit-cell parameters calculated from these data are: a = 10.130(8), b = 10.123(5), c = 21.107(13) Å, β = 102.28(5)° and V = 2115(2) $Å^3$.

Single-crystal XRD studies were carried out on a twinned crystal using a Bruker Smart Apex II DUO diffractometer equipped with a CCD detector (Cu$K\alpha$ radiation). The structure model was obtained by the dual space method and refined to R = 0.206 on the basis of 2107 independent reflections with $I > 2\sigma(I)$ (Table 3) using a *SHELX*-2014 software package (Sheldrick, 2015). Coordinates and thermal displacement parameters of atoms are given in Table 4, selected interatomic distances in Table 5.

Table 2. Powder X-ray diffraction data (d in Å) for elasmochloite.

I_{obs}	d_{obs}	I_{calc}*	d_{calc}	*hkl*
100	**10.33**	100	10.312	002
18	**7.04**	6, 4	7.077, 7.030	110, $\bar{1}$11
14	**6.33**	6, 3, 6	6.402, 6.310, 6.299	111, $\bar{1}$03, $\bar{1}$12
3	5.686	3	5.687	031
7	5.456	5	5.461	112
7	5.390	4	5.355	$\bar{1}$13
4	5.192	2	5.156	103
6	4.596	1, 2	4.594, 4.594	014, 113
7	4.508	2	4.506	$\bar{1}$14
5	4.285	2	4.284	$\bar{1}$22
4	4.132	5, 2	4.132, 4.109	202, $\bar{2}$13
7	4.073	10	4.076	023
5	4.027	5	4.023	$\bar{2}$04
2	3.990	4	3.990	122
4	3.830	1	3.826	212
24	**3.576**	13, 2	3.580, 3.569	$\bar{2}$21, $\bar{1}$24
13	**3.397**	4, 3, 2	3.437, 3.402, 3.361	006, 221, $\bar{2}$23
7	3.250	2, 1, 1	3.255, 3.243, 3.241	016, 204, 124
6	3.197	2	3.198	025
4	3.004	1	3.004	$\bar{1}$07
13	**2.966**	8	2.968	223
14	**2.920**	10	2.914	$\bar{2}$25
6	2.764	3	2.764	320
7	2.639	2	2.640	$\bar{3}$24
2	2.580	2	2.558	322
14	**2.529**	6, 5	2.532, 2.531	$\bar{4}$02, 040
12	**2.505**	14	2.504	225
14	**2.460**	2, 3, 11	2.475, 2.458, 2.455	400, 042, $\bar{2}$27
3	2.199	1	2.197	$\bar{3}$35
3	2.116	1	2.112	227
2	2.083	1	2.073	$\bar{2}$29
2	1.840	1	1.838	147
2	1.808	1	1.806	048
7	1.788	4, 2	1.790, 1.769	$\bar{4}$42, 440
3	1.758	1	1.758	$\bar{4}$44
2	1.720	1	1.720	345
3	1.602	1	1.599	0.4.10
2	1.542	1	1.541	621
3	1.520	1, 1	1.525, 1.518	$\bar{2}$65, $\bar{6}$27
2	1.467	1	1.466	623
2	1.459	1	1.456	265
2	1.446	1	1.446	$\bar{2}$67
2	1.433	1	1.437	3.2.11

*For the calculated pattern, only reflections with intensities ≥1 are given. The strongest reflections are marked in bold type.

Table 3. Crystal data, data collection information and structure-model refinement details for elasmochloite.

Crystal data	
Formula	$Na_3Cu_6BiO_4(SO_4)_5$
Crystal size (mm)	0.003 × 0.003 × 0.02
Crystal system, space group	Monoclinic, $P2_1/n$
a (Å)	10.1273(9)
b (Å)	10.1193(8)
c (Å)	21.1120(16)
β (°)	102.272(8)
V (Å^3)	2114.1(3)
Z	4
Data collection	
Instrument	Bruker Smart APEX DUO (CCD)
Radiation	Cu$K\alpha$ (λ = 1.54178 Å)
Temperature (K)	293(2)
2θ range (°)	8–136
Total collected reflections	3930
Independent reflections	2397
Independent observed $I > 2\sigma(I)$	2107
$R_{int.}$	0.120
R_σ	0.005
hkl range	$h = -12 \rightarrow 12$; $k = -9 \rightarrow 12$; $l = -14 \rightarrow 25$
Structure model solution and refinement	
Structure solution	Single component twin domain
Twin matrix	$\bar{1}$ 0 0/0 $\bar{1}$ 0 / 1 0 1
Reflection file type	HKLF4
Number of parameters	292
Number of restraints	86
R_1 [$F > 4\sigma(F)$], R_1 (all)	0.206, 0.216
wR_2 [$F > 4\sigma(F)$], wR_2 (all)	0.539, 0.555
$S = GoF$	2.77
$\Delta\sigma_{min}$, $\Delta\sigma_{min}$ (e Å^{-3})	−3.19, 7.45

7. Discussion

7.1. Crystal structure

The single-crystal XRD study of elasmochloite detected that all tested crystals are somewhat curved and represent micro-twins (twin matrix $\bar{1}$ 0 0/0 $\bar{1}$ 0/1 0 1). The observed twinning is a consequence of pseudo-tetragonal symmetry of the mineral (pseudo-tetragonal cell metrics is: a = 10.1 and c = 41.2 Å). The Cu$K\alpha$ radiation was chosen for achieving better angular separation of twin domains; however, even with Cu$K\alpha$, 65–70 % of reflections were found to be overlapped. Merging twin domains into HKLF5 reflection file did not result in an acceptable structure solution. Therefore, we applied single-domain integration using a very narrow integration box. Under these conditions, the collected data could be acceptably integrated (Table 3). The crystal structure has been solved (Table 4) but even the best refinement runs resulted in R_1 = 0.206 (Table 3). Thus, we consider our data only as a crystal-structure model. Nevertheless, the reliable values of thermal displacement parameters and interatomic distances (Tables 4 and 5), good values of bond-valence sums (calculated using bond-valence parameters reported by Gagné & Hawthorne, 2015: see Tables S1 and S2 in Supplementary Material, linked to this article and freely available at https://pubs.geoscienceworld.org/eurjmin), good agreement between measured and calculated powder XRD patterns (Table 2), zero charge balance in the structural formula and its agreement with electron microprobe data (Table 1), as well as the excellent value of the Gladstone-Dale compatibility index (Mandarino, 1981) confirms that the crystal structure model is correct.

Elasmochloite demonstrates a novel structure type. It possesses an original layered structure containing two types of polyhedral layers alternating along the **c** axis: (1) "copper-bismuth slabs" composed by [BiO_4O_2] polyhedra, [CuO_5] square pyramids and [CuO_4] squares and (2) "sodium slabs" consisting of [NaO_5] and [NaO_6] polyhedra (Fig. 4).

Table 4. Fractional atomic coordinates and isotropic displacement parameters ($Å^2$) for elasmochloite.

Site	*x*	*y*	*z*	U_{iso}
Bi	0.50882(15)	0.38416(18)	0.76717(7)	0.0511(11)
Cu1	0.6855(7)	0.3855(6)	0.6568(4)	0.0573(19)
Cu2	0.4554(7)	0.1530(7)	0.6593(3)	0.0563(17)
Cu3	0.2332(8)	0.3739(7)	0.6548(4)	0.0609(19)
Cu4	0.4620(9)	0.6057(7)	0.6543(4)	0.062(2)
Cu5	0.2519(7)	0.1313(6)	0.7600(4)	0.057(2)
Cu6	0.7461(7)	0.1351(7)	0.7459(4)	0.060(2)
Na1	0.915(2)	0.370(3)	0.5713(13)	0.082(7)
Na2	0.405(3)	0.871(3)	0.5635(11)	0.093(9)
Na3	0.9033(19)	−0.123(2)	0.5301(14)	0.073(6)
S1	0.6972(16)	0.1105(12)	0.5966(7)	0.071(4)
S2	0.1611(14)	0.0971(14)	0.6141(6)	0.065(3)
S3	0.1626(12)	0.6430(15)	0.5908(6)	0.061(3)
S4	0.7167(13)	0.6563(13)	0.6062(6)	0.066(3)
S5	0.4972(13)	0.8805(12)	0.7535(7)	0.064(4)
O1	0.603(2)	0.264(2)	0.7069(11)	0.035(4)
O2	0.343(4)	0.242(3)	0.714(3)	0.100(17)
O3	0.367(4)	0.506(4)	0.7055(17)	0.088(14)
O4	0.614(2)	0.510(3)	0.7084(10)	0.042(5)
O5	0.789(3)	0.692(4)	0.6719(11)	0.066(8)
O6	0.122(5)	0.067(6)	0.6765(13)	0.17(3)
O7	0.744(4)	0.518(4)	0.5966(18)	0.068(8)
O8	0.706(4)	0.256(2)	0.5911(18)	0.068(8)
O9	0.630(4)	0.833(8)	0.791(3)	0.14(2)
O10	0.553(2)	0.087(2)	0.5952(13)	0.056(8)
O11	0.301(2)	0.073(4)	0.607(2)	0.074(10)
O12	0.556(3)	0.983(3)	0.7192(15)	0.059(7)
O13	0.131(5)	0.240(2)	0.606(3)	0.106(17)
O14	0.142(3)	0.495(3)	0.5878(16)	0.061(7)
O15	0.434(7)	0.953(7)	0.800(3)	0.13(2)
O16	0.298(4)	0.664(4)	0.5851(19)	0.069(8)
O17	0.570(2)	0.683(3)	0.6007(18)	0.067(8)
O18	0.437(7)	0.780(4)	0.705(2)	0.12(2)
O19	0.143(3)	0.700(4)	0.6519(16)	0.067(9)
O20	0.775(5)	0.717(4)	0.5555(12)	0.109(18)
O21	0.072(6)	0.722(3)	0.536(3)	0.12(2)
O22	0.081(4)	0.015(4)	0.5614(17)	0.064(7)
O23	0.731(6)	0.054(6)	0.5372(19)	0.107(15)
O24	0.779(3)	0.061(3)	0.6571(12)	0.060(7)

Table 5. Selected interatomic distances (Å) for elasmochloite.

Bond	Distance	Bond	Distance	Bond	Distance
Na1–O7	2.44(4)	Cu2–O1	1.97(2)	S1–O8	1.477(19)
Na1–O8	2.53(4)	Cu2–O2	2.00(5)	S1–O10	1.476(19)
Na1–O13	2.52(4)	Cu2–O10	1.95(3)	S1–O23	1.48(2)
Na1–O14	2.59(4)	Cu2–O11	1.89(3)	S1–O24	1.454(19)
Na1–O15	2.94(8)	Cu2–O12	2.25(3)		
Na1–O21	2.47(7)				
Na2–O10	2.65(4)	Cu3–O2	1.99(3)	S2–O6	1.48(2)
Na2–O11	2.57(4)	Cu3–O3	2.04(3)	S2–O11	1.477(18)
Na2–O16	2.44(5)	Cu3–O13	1.87(3)	S2–O13	1.484(19)
Na2–O17	2.54(4)	Cu3–O14	1.95(3)	S2–O22	1.48(4)
Na2–O23	2.40(6)	Cu3–O15	2.26(6)		
Na3–O20	2.21(3)	Cu4–O3	1.89(2)	S3–O14	1.51(4)
Na3–O21	2.31(5)	Cu4–O4	1.96(2)	S3–O16	1.42(4)
Na3–O22	2.26(4)	Cu4–O16	2.05(4)	S3–O19	1.46(3)
Na3–O22	2.25(4)	Cu4–O17	1.90(4)	S3–O21	1.54(4)
Na3–O23	2.53(6)	Cu4–O18	2.11(4)		
Bi–O1	2.13(2)	Cu5–O2	1.86(5)	S4–O5	1.471(19)
Bi–O2	2.31(4)	Cu5–O3	1.99(4)	S4–O7	1.45(4)
Bi–O3	2.12(5)	Cu5–O6	2.07(4)	S4–O17	1.486(19)
Bi–O4	2.20(2)	Cu5–O19	2.06(4)	S4–O20	1.466(19)
Bi–O5	2.91(4)				
Bi–O6	2.70(4)				
Cu1–O1	1.92(2)	Cu6–O1	1.99(2)	S5–O9	1.48(2)
Cu1–O4	1.91(3)	Cu6–O4	1.99(2)	S5–O12	1.464(18)
Cu1–O7	2.02(4)	Cu6–O5	1.93(3)	S5–O15	1.48(2)
Cu1–O8	1.95(3)	Cu6–O12	2.43(3)	S5–O18	1.477(19)
Cu1–O9	2.03(5)	Cu6–O24	2.11(3)		

Corner-sharing [SO_4] tetrahedra integrate cationic polyhedra into the whole structure. The Bi atom possesses [4 + 2] coordination environment: bismuth-capped [BiO_4] square pyramid with two additional, long Bi–O bonds (Fig. 5A). A similar Bi coordination has been reported in tavagnascoite $Bi_4O_4(SO_4)(OH)_2$ (Bindi *et al.*, 2016) and several synthetic compounds containing bismuth oxido-clusters (Thurston *et al.*, 2005; Mehring *et al.*, 2006; Andrews *et al.*, 2008, 2012). In case of elasmochloite, there is an oxido-cluster [$BiCu_4O_{18}$] which gathers the [BiO_4] square pyramid with a ring consisting of four corner-sharing [CuO_5] square pyramids (Fig. 5b and c).

Five-fold coordinated Na is relatively uncommon but known in a series of minerals and inorganic compounds, *e.g.*, in makatite $Na_2Si_4O_8(OH)_2(H_2O)_4$ (Annehed *et al.*, 1982), lovdarite $K_4Na_{12}(Be_8Si_{28}O_{72})\cdot 18H_2O$ (Merlino, 1990) and the synthetic phases $Na_2MoO_4\cdot 2H_2O$ (Matsumoto *et al.*, 1975), Na_4SiO_4 (Baur *et al.*, 1986), $NaY(SeO_3)_2$ (Morris *et al.*, 1990), and α-NaB_3O_5 (Krogh-Moe, 1974).

Representation of the crystal structure using an anion-centred approach (Krivovichev *et al.*, 2013) (Fig. 6, Table 6) reveals relationships of elasmochloite with other Bi- and Te-bearing minerals having an additional oxygen atom: nabokoite $KCu_7Te^{4+}O_4(SO_4)_5Cl$ (Pertlik & Zemann, 1988), its likely structural analogue atlasovite, $KCu_7Fe^{3+}Bi^{3+}O_4(SO_4)_5Cl$ (Popova *et al.*, 1987; our unpublished data) and the recently described hydroxo-selenite favreauite $PbCu_6BiO_4(Se^{4+}O_3)_4(OH)\cdot H_2O$ (Mills *et al.*, 2014). The crystal structures of nabokoite and favreauite were analyzed and compared by Mills *et al.* (2014) who showed that both minerals contain the same oxycentred structural unit: a layer composed by edge-shared "half-cube" clusters [Cu_8BiO_4] of oxygen-centred tetrahedra. The same perforated layer of [Cu_8BiO_4] clusters, having tetragonal symmetry, can be found in elasmochloite (Fig. 6). However, in contrast with the structures of nabokoite and favreauite, successive [$Cu_8Bi(Te)O_4$] layers in the elasmochloite structure are shifted along the **a** axis (Fig. 6) resulting in monoclinic distortion of elasmochloite lattice.

7.2. Relationship to other species

Elasmochloite has no direct analogue in chemical or structural respect among both natural and synthetic compounds. It possesses unique chemical composition, unit-cell dimensions, powder XRD pattern and Raman spectrum.

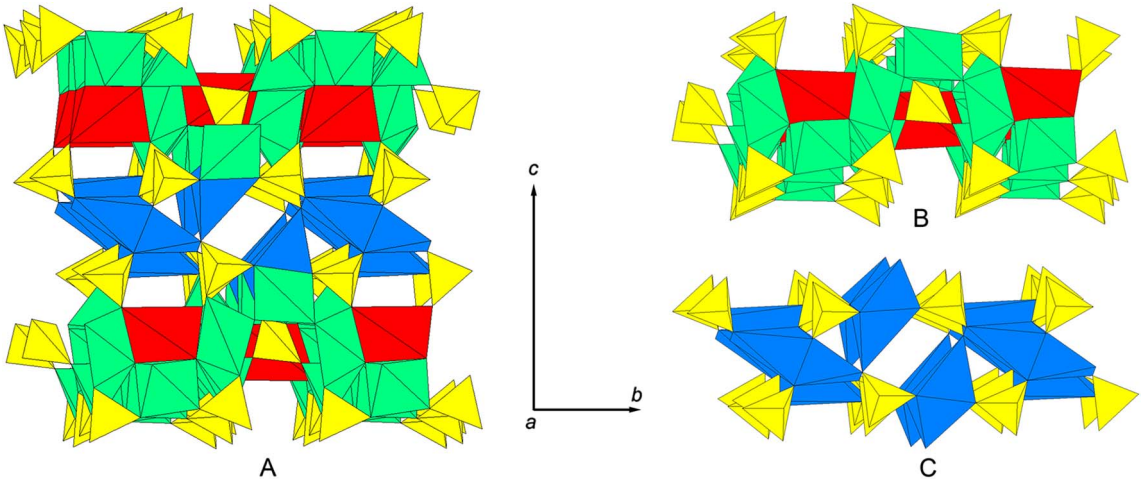

Figure 4. (a) General view of the elasmochloite structure, projection onto (100). Alternation of Cu–Bi–S–O layers composed by [BiO_4O_2], [CuO_5] and [CuO_4] polyhedra with Na–S–O layers consisting of [NaO_5] and [NaO_6] polyhedra connected *via* corner-sharing [SO_4] tetrahedra. (b) The Cu–Bi–S–O layer. (c) The Na–S–O layer. Legend: [BiO_4O_6] polyhedra are red, [CuO_5] and [CuO_4] polyhedra are green, [NaO_5] and [NaO_6] polyhedra are blue and [SO_4] tetrahedra are yellow.

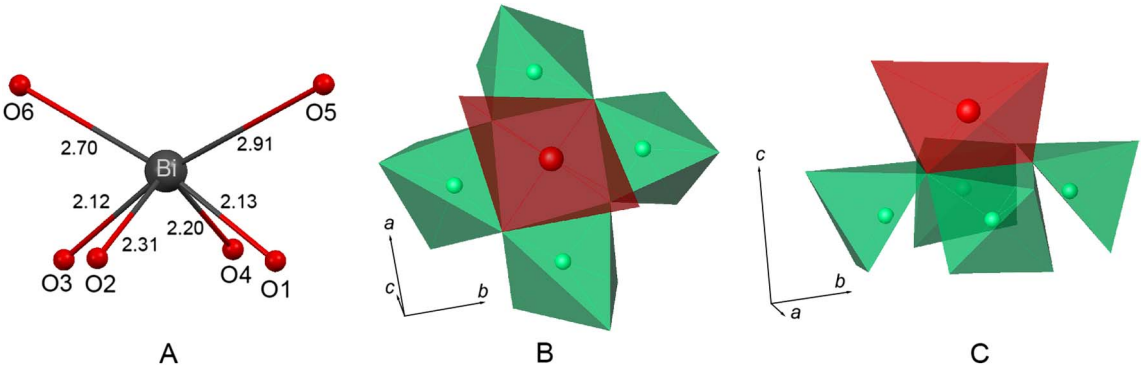

Figure 5. (a) Ball-and-stick representation of the [BiO_4O_2] polyhedron, which can be considered as a bismuth-capped square pyramid with two elongated Bi–O bonds. The O5 and O6 atoms are the corners of sulfate-ions whereas O1, O2, O3 and O4 form Bi–O–Cu bridges. Bi–O distances are given in Å. (b and c) Architecture of [$BiCu_4O_{18}$] cluster composed by a ring of corner-sharing [CuO_5] square pyramids (green) capped with edge-sharing [BiO_4O_2] polyhedron (red) (two projections).

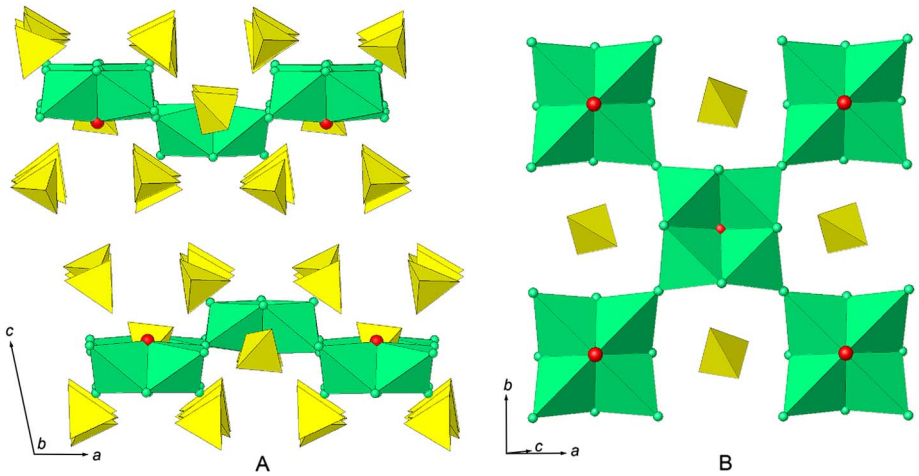

Figure 6. Crystal structure of elasmochloite in anion-centred representation. (a) Layers composed of edge-shared "half-cube" clusters [Cu_8BiO_4] of oxygen-centred tetrahedra. (b) Perforated layer of [Cu_8BiO_4] "half-cube" clusters. Sodium atoms have been omitted for clarity. Legend: Cu atom, green ball; Bi atom, red ball; [Cu_8BiO_4] cluster, green; [SO_4] terahedron, yellow.

Table 6. Interatomic distances (Å) in the [Cu_8BiO_4] cluster of elasmochloite.

Bond	Distance	Bond	Distance
O1–Bi1	2.13(2)	O3–Bi1	2.12(5)
O1–Cu1	1.92(2)	O3–Cu3	2.04(3)
O1–Cu2	1.97(2)	O3–Cu4	1.89(2)
O1–Cu6	1.99(2)	O3–Cu5	1.99(4)
O2–Bi1	2.31(4)	O4–Bi1	2.20(2)
O2–Cu2	2.00(5)	O4–Cu1	1.91(3)
O2–Cu3	1.99(3)	O4–Cu4	1.96(2)
O2–Cu5	1.86(5)	O4–Cu6	1.99(2)

Some minerals demonstrate a remote, firstly chemical relationship to elasmochloite. There are four Cu,Bi-oxysalts with additional O^{2-} anions. Atlasovite $KCu_6Fe^{3+}BiO_4(SO_4)_5Cl$ (Popova *et al.*, 1987) belongs to the same family of H-free alkali-copper oxysulfates (see Sect. 1). It is noteworthy that atlasovite (1) occurs in the same Arsenatnaya fumarole, (2) contains Bi^{3+} as a species-defining cation, (3) is tetragonal and (4) has the same sum of all atoms in the formula (39 *apfu*) and the same Cu:Bi:S:O = 6:1:5:24 ratios as elasmochloite $Na_3Cu_6BiO_4(SO_4)_5$. However, these minerals differ from one another in additional constituents, in crystal data, structure and physical properties. The crystal structure of atlasovite was not studied; however, it is most likely isostructural with nabokoite $KCu_7Te^{4+}O_4(SO_4)_5Cl$ (Pertlik & Zemann, 1988) and forms with it zoned crystals and a solid-solution series (Popova *et al.*, 1987; our unpublished data). These minerals are structurally close to the above discussed favreauite $PbCu_6BiO_4(Se^{4+}O_3)_4(OH)\cdot H_2O$, in which Bi^{3+} has eight-fold coordination (Mills *et al.*, 2014) as well as in another oxyselenite, francisite $Cu_3BiO_2(Se^{4+}O_3)_2Cl$ (Pring *et al.*, 1990). In mrázekite $Cu_3Bi_2O_2(PO_4)_2(OH)_2\cdot 2H_2O$, the Bi^{3+} cations demonstrate a [2 + 2] coordination with the one-side arrangement of ligands typical for cations with lone-pair electrons (Effenberger *et al.*, 1994). Favreauite, francisite and mrázekite, unlike the atlasovite–nabokoite series minerals and elasmochloite, have a supergene, low-temperature origin.

Acknowledgements: We thank two anonymous referees for their valuable comments. This work was supported by the Russian Science Foundation, grant no. 19-17-00050. The technical support by the SPbSU X-Ray Diffraction Resource Center is acknowledged.

References

Andrews, P.C., Junk, P.C., Nuzhnaya, I., Spiccia, L. (2008): Fluorinated bismuth alkoxides: from monomers to polymers and oxo-clusters. *Dalton Trans.*, 2557–2568.

Andrews, P.C., Busse, M., Junk, P.C., Forsyth, C.M., Peiris, R. (2012): Sulfonato-encapsulated bismuth(III) oxido-clusters from Bi_2O_3 in water under mild conditions. *Chem. Commun.*, **48**, 7583–7585.

Annehed, H., Fälth, L., Lincoln, F.J. (1982): Crystal structure of synthetic Makatite $Na_2Si_4O_8(OH)_2(H_2O)_4$. *Z. Kristallogr.*, **159**, 203–210.

Baur, W.H., Halwax, E., Völlenkle, H. (1986): Comparison of the crystal structures of sodium orthosilicate, Na_4SiO_4, and sodium orthogermanate, Na_4GeO_4. *Monatsh. Chem.*, **111**, 793–797.

Bindi, L., Biagioni, C., Martini, B., Salvetti, A., Fontana, G.D., Taronna, M., Ciriotti, M.E. (2016): Tavagnascoite, $Bi_4O_4(SO_4)(OH)_2$, a new oxyhydroxy bismuth sulfate related to klebelsbergite. *Mineral. Mag.*, **80**, 647–657.

Effenberger, H. & Zemann, J. (1984): The crystal structure of caratiite. *Mineral. Mag.*, **48**, 541–546.

Effenberger, H., Krause, W., Belendorff, K., Bernhardt, H.J., Medenbach, O., Hybler, J., Petříček, V. (1994): Revision of the crystal structure of mrázekite, $Bi_2Cu_3(OH)_2O_2(PO_4)_2\cdot 2H_2O$. *Can. Mineral.*, **32**, 365–372.

Fedotov, S.A. & Markhinin, Y.K., eds. (1983): The Great Tolbachik Fissure Eruption. Cambridge Univ. Press, New York, NY.

Gagné, O.C. & Hawthorne, F.C. (2015): Comprehensive derivation of bond-valence parameters for ion pairs involving oxygen. *Acta Crystallogr. B*, **71**, 562–578.

Gorskaya, M.G., Filatov, S.K., Rozhdestvenskaya, I.V., Vergasova, L.P. (1992): The crystal structure of klyuchevskite, $K_3Cu_3(Fe,Al)O_2(SO_4)_4$, a new mineral from Kamchatka volcanic sublimates. *Mineral. Mag.*, **56**, 411–416.

Gorskaya, M.G., Vergasova, L.P., Filatov, S.K., Rolich, D.V., Ananiev, V.V. (1995): Alumoklyuchevskite, $K_3Cu_3AlO_2(SO_4)_4$, a new oxysulfate of K, Cu and Al from volcanic exhalations, Kamchatka, Russia. *Zapiski VMO*, **124**, 95–100. (in Russian).

Krivovichev, S.V., Filatov, S.K., Cherepansky, P.N. (2009): The crystal structure of alumoklyuchevskite, $K_3Cu_3AlO_2(SO_4)_4$. *Geol. Ore Deposits*, **51**, 656–662.

Krivovichev, S.V., Mentre, O., Siidra, O.I., Colmont, M., Filatov, S.K. (2013): Anion-centered tetrahedra in inorganic compounds. *Chem. Rev.*, **113**, 6459–6535.

Krogh-Moe, J. (1974): The crystal structure of a sodium triborate, α-$Na_2O\cdot 3B_2O_3$. *Acta Crystallogr. B*, **30**, 747–752.

Mandarino, J.A. (1981): The Gladstone-Dale relationship. Part IV. The compatibility concept and its application. *Can. Mineral.*, **14**, 498–502.

Matsumoto, K., Kobayashi, A., Sasaki, Y. (1975): The crystal structure of sodium molybdate dihydrate, $Na_2MoO_4\cdot 2H_2O$. *Bull. Chem. Soc. Jpn.*, **48**, 1009–1013.

Mehring, M., Mansfeld, D., Paalasmaa, S., Schürmann, M. (2006): Polynuclear bismuth-oxo clusters: insight into the formation process of a metal oxide. *Chem. Eur. J.*, **12**, 1767–1781.

Merlino, S. (1990): Lovdarite, $K_4Na_{12}(Be_8Si_{28}O_{72})\cdot(18H_2O)$, a zeolite-like mineral: structural features and OD character. *Eur. J. Mineral.*, **2**, 809–817.

Mills, S.J., Kampf, A.R., Housley, R.M., Christy, A.G., Thorne, B., Chen, Y.-S., Steele, I.M. (2014): Favreauite, a new selenite mineral from the El Dragón mine, Bolivia. *Eur. J. Mineral.*, **26**, 771–781.

Morris, R.E., Hriljac, J.A., Cheetham, A.K. (1990): Synthesis and crystal structures of two novel selenites, $NaY(SeO_3)_2$ and $NaLa(SeO_3)_2$. *Acta Crystallogr. C*, **46**, 2013–2017.

Nakamoto, K. (1986): Infrared and Raman Spectra of Inorganic and Coordination Compounds. John Wiley & Sons, New York, NY.

Pekov, I.V., Zubkova, N.V., Yapaskurt, V.O., Belakovskiy, D.I., Chukanov, N.V., Lykova, I.S., Saveliev, D.P., Sidorov, E.G., Pushcharovsky, D.Y. (2014): Wulffite, $K_3NaCu_4O_2(SO_4)_4$, and parawulffite, $K_5Na_3Cu_8O_4(SO_4)_8$, two new minerals from fumarole sublimates of the Tolbachik volcano, Kamchatka, Russia. *Can. Mineral.*, **52**, 699–716.

Pekov, I.V., Zubkova, N.V., Agakhanov, A.A., Chukanov, N.V., Belakovskiy, D.I., Sidorov, E.G., Britvin, S.N., Pushcharovsky, D.Y. (2016): Eleomelanite, IMA 2015–118. CNMNC Newsletter No. 30, April 2016, page 412. *Mineral. Mag.*, **80**, 407–413.

Pekov, I.V., Koshlyakova, N.N., Zubkova, N.V., Lykova, I.S., Britvin, S.N., Yapaskurt, V.O., Agakhanov, A.A., Shchipalkina, N.V., Turchkova, A.G., Sidorov, E.G. (2018a): Fumarolic arsenates – a special type of arsenic mineralization. *Eur. J. Mineral.*, **30**, 305–322.

Pekov, I.V., Zubkova, N.V., Agakhanov, A.A., Pushcharovsky, D.Y., Yapaskurt, V.O., Belakovskiy, D.I., Vigasina, M.F., Sidorov, E.G., Britvin, S.N. (2018b): Cryptochalcite $K_2Cu_5O(SO_4)_5$ and cesiodymite $CsKCu_5O(SO_4)_5$ – two new isotypic minerals and the K–Cs isomorphism in this solid-solution series. *Eur. J. Mineral.*, **30**, 593–607.

Pekov, I.V., Zubkova, N.V., Pushcharovsky, D.Y. (2018c): Copper minerals from volcanic exhalations – a unique family of natural compounds: crystal chemical review. *Acta Crystallogr. B*, **74**, 502–518.

Pertlik, F. & Zemann, J. (1988): The crystal structure of nabokoite, $Cu_7TeO_4(SO_4)_5{\cdot}KCl$: the first example of a $Te(IV)O_4$ pyramid with exactly tetragonal symmetry. *Mineral. Petrol.*, **38**, 291–298.

Popova, V.I., Popov, V.A., Rudashevskiy, N.S., Glavatskikh, S.F., Polyakov, V.O., Bushmakin, A.F. (1987): Nabokoite $Cu_7TeO_4(SO_4)_5{\cdot}KCl$ and atlasovite $Cu_6Fe^{3+}Bi^{3+}O_4(SO_4)_5{\cdot}KCl$. New minerals of volcanic exhalations. *Zapiski VMO*, **116**, 358–367. (in Russian).

Pring, A., Gatehouse, B.M., Birch, W.D. (1990): Francisite, $Cu_3Bi(SeO_3)_2O_2Cl$, new mineral from Iron Monarch, South Australia: description and crystal structure. *Am. Mineral.*, **75**, 1421–1425.

Scordari, F. & Stasi, F. (1990): The crystal structure of euchlorine, $NaKCu_3O(SO_4)_3$. *N. Jb. Mineral. Mh.*, **1990**, 241–253.

Sheldrick, G.M. (2015): Crystal structure refinement with SHELXL. *Acta Crystallogr. C*, **71**, 3–8.

Siidra, O.I., Nazarchuk, E.V., Zaitsev, A.N., Lukina, E.A., Avdontseva, E.Y., Vergasova, L.P., Vlasenko, N.S., Filatov, S.K., Turner, R., Karpov, G.A. (2017): Copper oxosulphates from fumaroles of Tolbachik volcano: puninite, $Na_2Cu_3O(SO_4)_3$ – a new mineral species and structure refinements of kamchatkite and alumoklyuchevskite. *Eur. J. Mineral.*, **28**, 499–510.

Starova, G.L., Filatov, S.K., Fundamensky, V.S., Vergasova, L.P. (1991): The crystal structure of fedotovite, $K_2Cu_3O(SO_4)_3$. *Mineral. Mag.*, **55**, 613–616.

Thurston, J.H., Swenson, D.C., Messerle, L. (2005): Solvolytic routes to new nonabismuth hydroxy- and alkoxy-oxo complexes: synthesis, characterization and solid-state structures of novel nonabismuth polyoxo cations $Bi_9(\mu_3\text{-}O)_8(\mu 3-OR)_6^{5+}$ (R = H, Et). *Chem. Commun.*, **33**, 4228–4230.

Varaksina, T.V., Fundamensky, V.S., Filatov, S.K., Vergasova, L.P. (1990): The crystal structure of kamchatkite, a new naturally occurring oxychloride sulphate of potassium and copper. *Mineral. Mag.*, **54**, 613–616.

Vergasova, L.P., Filatov, S.K., Serafimova, E.K., Starova, G.L. (1984): Piypite, $K_2Cu_2O(SO_4)_2$, a new mineral of volcanic exhalations. *Dokl. AN SSSR*, **275**, 714–717. (in Russian).

Vergasova, L.P., Filatov, S.K., Serafimova, E.K., Starova, G.L. (1988a): Fedotovite, $K_2Cu_3O(SO_4)_3$, a new mineral of volcanic exhalations. *Dokl. AN SSSR*, **299**, 961–964. (in Russian).

Vergasova, L.P., Filatov, S.K., Serafimova, E.K., Varaksina, T.V. (1988b): Kamchatkite, $KCu_3OCl(SO_4)_2$, a new mineral of volcanic sublimates. *Zapiski VMO*, **117**, 459–461. (in Russian).

Vergasova, L.P., Filatov, S.K., Gorskaya, M.G., Ananiev, V.V., Sharov, A.S. (1989): Klyuchevskite, $K_3Cu_3(Fe,Al)O_2(SO_4)_4$, a new mineral from volcanic exhalations. *Zapiski VMO*, **118**, 70–73. (in Russian).

Received 20 May 2019
Modified version received 16 July 2019
Accepted 25 July 2019